

# Computer modelling of the origin of defects in ceramic injection moulding

## Part II *Shrinkage voids*

K. N. HUNT, J. R. G. EVANS

*Department of Materials Technology, Brunel University, Uxbridge, Middlesex, UK*

J. WOODTHORPE

*T & N Technology, Cawston House, Cawston, Rugby, UK*

Using the thermal properties previously acquired for a polystyrene–zirconia suspension, the solidification and shrinkage of injection-moulded rectangular bars was computed by a finite difference numerical method. By considering the final stage of mould packing, upper and lower bounds for the moulding conditions needed to avoid internal shrinkage defects and sink marks were successfully predicted. The resulting computer method allows the influence of a wide range of material and machine parameters to be explored.

### 1. Introduction

The ceramic injection moulding process involves a sequence of operations [1, 2] each of which is capable of introducing defects [3] which cannot subsequently be removed. At the solidification stage in the mould cavity, voids and cracks are often observed in thick sections [4, 5] and under suitable conditions the “sink” marks characteristic of unfilled polymer injection moulding may occur. Voids are a consequence of the fall in pressure in the interior of the moulding after solidification of the sprue [6] at a stage when the rigidity of the walls of the moulding inhibits “sinking” deformation. In the present work their origin is explained quantitatively by reference to the properties of a polystyrene–zirconia injection moulding suspension. Cracks originate from residual stresses generated after solidification and these will be analysed in a subsequent section [7]. The thermal properties and equation of state needed to execute these computer predictions have been reported previously [8]. The procedure for obtaining the sprue closure time by a finite difference unsteady state method and the significance of sprue closure time will be discussed elsewhere [9].

The objective of this work was to prepare numerical models to simulate the complex sequence of processes occurring during the solidification of ceramic suspensions in the mould cavity. Such models are of little value until validated by appeal to experiment. The present work therefore compares the predicted incidence of voids with the results of an experimental injection moulding programme. In order for such work to be of use to a wide range of practitioners, it is inevitable that simplifications to the model must be made and these are discussed. The value in such work lies in its predictive potential made possible by the

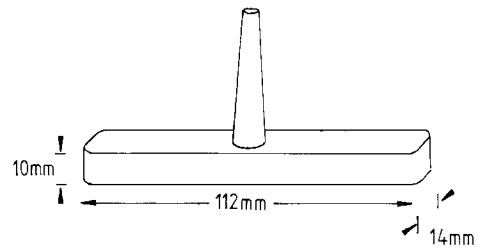


Figure 1 Dimensions of the rectangular bar.

facility to execute large numbers of “experiments” on a computer in order to investigate the effect of material and machine parameters on the quality of mouldings.

### 2. Experimental methods

The injection moulding suspension was prepared by the method given in Part I [8] and was identical in composition. A Sandretto 6GV/50 reciprocating screw machine was used to injection mould the rectangular bars shown in Fig. 1 with the settings given in Table I. Three series of bars were prepared with conditions specified in Table II. The sprue diameter refers to

TABLE I Injection moulding conditions for rectangular bars

Screw rotation speed	150 r.p.m.
Dose stop position	$9.0 \times 10^{-5} \text{ m}^3$
Decompression stop position	$9.5 \times 10^{-5} \text{ m}^3$
Feed zone temperature	190 °C
Mid zone temperature	200 °C
Metering zone temperature	210 °C
Nozzle temperature	220 °C
Nominal injection speed	$1.44 \times 10^{-4} \text{ m}^{-3} \text{ sec}^{-1}$
Total injection time	90 sec
Mould temperature	See Table II
Sprue size	See Table II

the narrow end and the cone semi-angles were 2.1° and 1.6° for the large and small sprues, respectively. A Cole's W3/3393 mould heater was used to maintain mould temperature. The cavity was fitted with a Dynisco FT444DH force transducer with a range of 4400N. All moulded bars were X-ray radiographed using a Macrotank K X-ray unit.

### 3. Computation

#### 3.1. Calculation of residual pressure in a long rectangular bar

The heat flow equation in two dimensions may be written as

$$\frac{1}{\alpha} \frac{\partial T}{\partial t} = \frac{\partial^2 T}{\partial x^2} + \frac{\partial^2 T}{\partial y^2} \quad (1)$$

where  $\alpha$  is the thermal diffusivity. This was cast in its Crank–Nicolson form [10],

$$\begin{aligned} & \frac{1}{\alpha} \frac{T(x, y, t + \Delta t/2) - T(x, y, t)}{\Delta t/2} \\ &= \frac{T(x + \Delta x, y, t + \Delta t/2) - 2T(x, y, t + \Delta t/2) + T(x - \Delta x, y, t + \Delta t/2)}{\Delta x^2} \\ &+ \frac{T(x, y + \Delta y, t) - 2T(x, y, t) + T(x, y - \Delta y, t)}{\Delta y^2} \end{aligned} \quad (3a)$$

and

$$\begin{aligned} & \frac{1}{\alpha} \frac{T(x, y, t + \Delta t) - T(x, y, t + \Delta t/2)}{\Delta t/2} \\ &= \frac{T(x + \Delta x, y, t + \Delta t/2) - 2T(x, y, t + \Delta t/2) + T(x - \Delta x, y, t + \Delta t/2)}{\Delta x^2} \\ &+ \frac{T(x, y + \Delta y, t + \Delta t) - 2T(x, y, t + \Delta t) + T(x, y - \Delta y, t + \Delta t)}{\Delta y^2} \end{aligned} \quad (3b)$$

$$\begin{aligned} & T(x, y, t + \Delta t) - T(x, y, t) = \\ & \frac{1}{2} r_x [T(x + \Delta x, y, t + \Delta t) - 2T(x, y, t + \Delta t) \\ & + T(x - \Delta x, y, t + \Delta t) + T(x + \Delta x, y, t) \\ & - 2T(x, y, t) + T(x - \Delta x, y, t)] \\ & + \frac{1}{2} r_y [T(x, y + \Delta y, t + \Delta t) \\ & - 2T(x, y, t + \Delta t) + T(x, y - \Delta y, t + \Delta t) \\ & + T(x, y + \Delta y, t) - 2T(x, y, t) \\ & + T(x, y - \Delta y, t)] \end{aligned}$$

where

$$r_x = \alpha \frac{\Delta t}{\Delta x^2} \quad \text{and} \quad r_y = \alpha \frac{\Delta t}{\Delta y^2}. \quad (2)$$

This was solved using the alternating direction implicit method (ADI) [10, 11]. Equation 2 was rewritten as two equations with time steps  $\Delta t/2$ . The first equation (3a) is implicit only in the  $x$  direction and the second (3b) is implicit only in the  $y$  direction.

Due to symmetry only one quarter of the bar cross-section need be considered for calculation. Energy balance equations were written for the various boundary nodes [10]. For example, considering the point shown in Fig. 2.

$$\begin{aligned} & \frac{1}{\alpha} \frac{\Delta x \Delta y}{2} \left( \frac{T(i, n, t + \Delta t) - T(i, n, t)}{\Delta t} \right) \\ &= -\Delta x \left( \frac{T(i, n, t) - T(i, n - 1, t)}{2\Delta y} + \frac{T(i, n, t + \Delta t) - T(i, n - 1, t + \Delta t)}{2\Delta y} \right) \\ & - \frac{h \Delta x}{2} (T(i, n, t) + T(i, n, t + \Delta t) - 2T_m) \\ & + \frac{\Delta y}{2} \left( \frac{T(i + 1, n, t) - T(i, n, t)}{2\Delta x} + \frac{T(i + 1, n, t + \Delta t) - T(i, n, t + \Delta t)}{2\Delta x} \right) \\ & - \frac{\Delta y}{2} \left( \frac{T(i, n, t) - T(i - 1, n, t)}{2\Delta x} + \frac{T(i, n, t + \Delta t) - T(i - 1, n, t + \Delta t)}{2\Delta x} \right) \end{aligned} \quad (4)$$

where general points  $(i, j)$  have values between 0 on the centre lines and  $n$  at the mould wall interface and  $T_m$  is the mould temperature.

This was written in its alternating direction implicit

TABLE II Variable injection moulding conditions for rectangular bars

	Series		
	1	2	3
Sprue diameter (mm)	6.9	6.9	10.0
Mould temperature (°C)	25	46	25
Injection pressure = hold pressure (MPa)	10–100 variable		

form

$$\begin{aligned} & \frac{1}{\alpha} \frac{\Delta x \Delta y}{2} \left( \frac{T(i, n, t + \Delta t/2) - T(i, n, t)}{\Delta t} \right) \\ &= \frac{\Delta y}{2} \left( \frac{T(i + 1, n, t + \Delta t/2) - T(i, n, t + \Delta t/2)}{2\Delta x} \right) \\ & \quad - \frac{\Delta y}{2} \left( \frac{T(i, n, t + \Delta t/2) - T(i - 1, n, t + \Delta t/2)}{2\Delta x} \right) \\ & \quad - \Delta x \left( \frac{T(i, n, t) - T(i, n - 1, t)}{2\Delta y} \right) \\ & \quad - \frac{h\Delta x}{k} \frac{\Delta x}{2} (T(i, n, t) - T_m) \end{aligned}$$

and

$$\begin{aligned} & \frac{1}{\alpha} \frac{\Delta x \Delta y}{2} \left( \frac{T(i, n, t + \Delta t) - T(i, n, t + \Delta t/2)}{\Delta t} \right) \\ &= \frac{\Delta y}{2} \left( \frac{T(i + 1, n, t + \Delta t/2) - T(i, n, t + \Delta t/2)}{2\Delta x} \right) \\ & \quad - \frac{\Delta y}{2} \left( \frac{T(i, n, t + \Delta t/2) - T(i - 1, n, t + \Delta t/2)}{2\Delta x} \right) \\ & \quad - \Delta x \left( \frac{T(i, n, t + \Delta t) - T(i, n - 1, t + \Delta t)}{2\Delta y} \right) \\ & \quad - \frac{h\Delta x}{k} \frac{\Delta x}{2} (T(i, n, t + \Delta t) - T_m) \end{aligned} \quad (5)$$

Similar equations were written for the other boundary points. These were rewritten as pairs of equations in the same manner as Equation 3 for solution by the ADI method.

Thus two equations involving tridiagonal matrices were derived, one for heat flow in the  $x$  direction which was solved for the time step  $t$  to  $t + \Delta t/2$ , followed by one for heat flow in the  $y$  direction for the time step  $t + \Delta t/2$  to  $t + \Delta t$ .

The heat transfer coefficient  $h$  was taken as  $1000 \text{ W m}^{-1} \text{ K}^{-1}$  [5, 12, 13]. Mills [14] has suggested that  $h$  varies between approximately 1000 and  $100 \text{ W m}^{-1} \text{ K}^{-1}$  as pressure decreases. Values as low as  $150 \text{ W m}^{-1} \text{ K}^{-1}$  have been proposed by other workers for the moulding of polymers [15, 16]. Direct measurements of  $h$  applicable to the problem of injection moulding are difficult to acquire.

Prior to sprue solidification, the hydrostatic pressure in the cavity was taken to be the maximum pressure recorded on the cavity pressure transducer just after mould filling. In the absence of a cavity

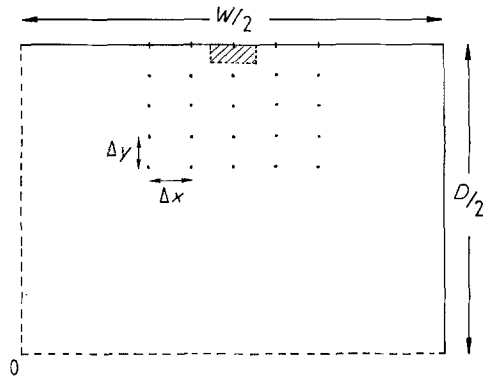


Figure 2 The finite difference mesh used for two-dimensional heat flow in a long rectangular bar.

pressure transducer this value could be obtained from the hold pressure set by the machine. In practice, however, there is a pressure defect associated with the inefficiency of pressure transmission through the suspension and can be substantial [5]. In the present work the pressure defect was 6 MPa when the injection pressure was set at 20 MPa rising to 20 MPa for an injection pressure of 100 MPa. A plot of cavity pressure as a function of set pressure on material is shown in Fig. 3. Clearly reliance on set pressure is subject to the accuracy of the proportional pressure relief valve on individual machines.

The specific volume of each segment was considered to fall freely as the temperature decreased and as material continued to fill the core under a constant pressure. At the time when the sprue solidified, the specific volume of each segment was calculated and the average specific volume of the sealed pocket of fluid contained within the core of the moulding was found. As no more material can flow into the moulding, the mass of material in the core region remained constant. The solidified walls of the moulding were assumed to be rigid so that the volume of material in the core was taken to be constant. In fact the walls of the moulding continue to contract as cooling proceeds but the cubical coefficient of thermal expansion in the solid state was  $1.35 \times 10^{-4} \text{ }^\circ\text{C}^{-1}$ , [8], compared with

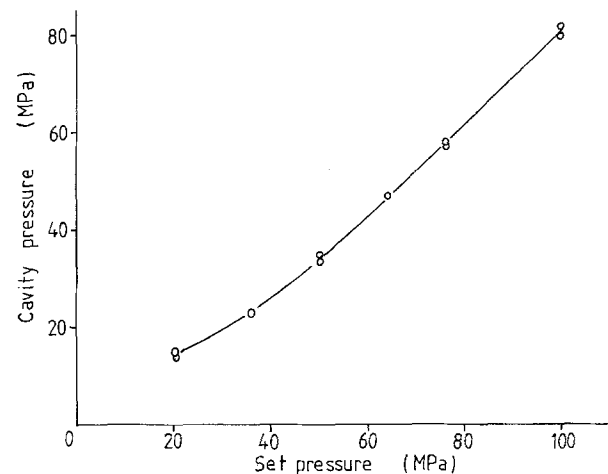


Figure 3 Measured cavity pressure as a function of set pressure on material for a mould temperature of 25 °C.

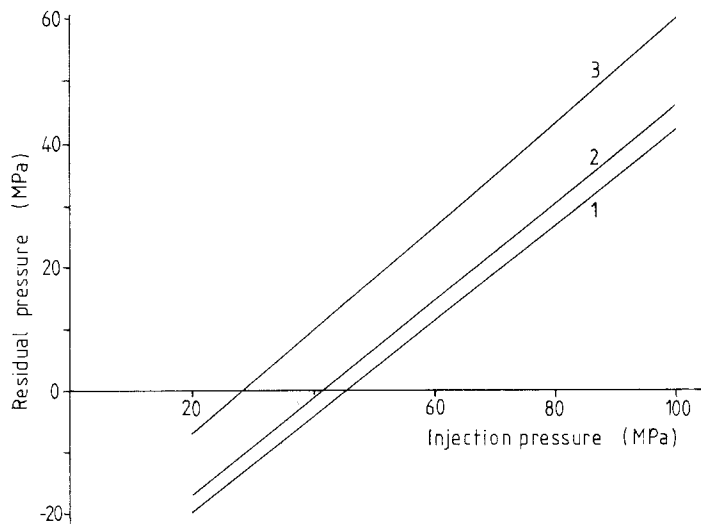


Figure 4 Predicted residual pressure as a function of injection pressure for series 1, 2 and 3 mouldings obtained using calculated sprue solidification times.

$2.97 \times 10^{-4} \text{ } ^\circ\text{C}^{-1}$  for the liquid. Since  $T_g$  was  $58 \text{ } ^\circ\text{C}$  the shrinkage in the solid state as the temperature range of  $33 \text{ } ^\circ\text{C}$  is traversed is small relative to the shrinkage of the fluid from the injection temperature of  $220 \text{ } ^\circ\text{C}$ . This simplification may not be valid for suspensions based on high melting point polymers.

Since the mass in the core was constant and the volume of the core was assumed constant, the average specific volume of material in the core was considered constant. A residual pressure was then calculated from the Spencer and Gilmore equation of state previously derived [8] using the average specific volume of the core and setting the temperature equal to  $T_g$ . The number of space steps was set at  $15 \times 15$  for one quarter of the bar section and the time step was taken as the gate freeze-off time divided by 100. The program was written in BASIC and had a run time of approximately 20 min on Opus and Amstrad personal computers.

The edge temperatures were seen to oscillate as a function of time during computation and these oscillations were damped by setting edge temperatures equal to the average edge temperature after each time step  $\Delta t$ . The justification for this procedure was that, provided the surface heat transfer coefficient was large, the variation of temperature along the edge of the moulded bar would be small. Results obtained by decreasing the time step by a factor of 10 showed that these oscillations did not affect the results. The nodes at the edge of the bar were not considered when calculating the pressure.

## 4. Results and discussion

### 4.1. Comparison of initial predictions with experiment

Rectangular bars were injection moulded with conditions given in Tables I and II with all variables fixed except the injection and hold pressures. These were kept equal and their value was systematically varied. All the bars were X-ray radiographed to ascertain the extent of internal voiding.

The material properties previously obtained [8] and the injection moulding conditions described were used for computation of residual pressure. In the first

series of calculations sprue closure time was calculated by a pure implicit finite difference method described elsewhere [9] as the time taken for the axis of the sprue to reach the glass transition temperature of the suspension, namely  $58 \text{ } ^\circ\text{C}$ . For the three series of moulding conditions shown in Tables I and II these times were predicted to be 25, 35 and 48 sec, respectively.

The injection pressure above which no voids were seen could then be compared with the predictions of the model. The calculated residual pressure was plotted as a function of injection and hold pressure for the three series of moulding conditions and the results are shown in Fig. 4. The predicted injection pressure at which residual pressure falls to zero may be compared with the results of radiographs of moulded bodies. Fig. 5 shows prints of radiographs of series 1 mouldings at 24, 32, 57 and 80 MPa. Table III summarizes these comparisons. In general, the computer predictions slightly underestimate the initial cavity pressure needed to prevent the formation of voids, however, bearing in mind the need to simplify a very complex physical problem in order to make the computation manageable and widely usable, this initial agreement

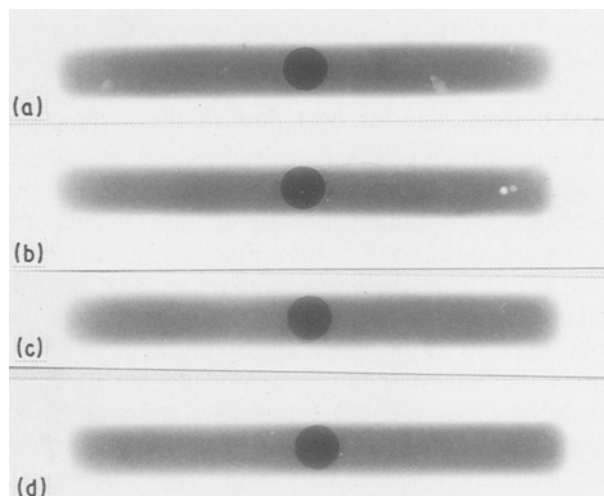


Figure 5 Prints of X-ray radiograph of bars from series 1 prepared with various injection pressures. (a) 24 MPa, (b) 32 MPa, (c) 57 MPa, (d) 80 MPa.

TABLE III Comparison of calculated and experimental residual pressures for nucleation of voids

Moulding series	Injection pressure for void-free mouldings		Calculated <sup>a</sup> (MPa)	Experimental <sup>b</sup> (MPa)	Calculated <sup>c</sup> (MPa)
	Sprue diameter (mm)	Mould temperature (°C)			
1	6.9	25	45	between 57 and 80	75
2	6.9	46	41	between 35 and 56	77
3	10	25	28	between 33 and 47	57

<sup>a</sup>Using sprue solidification time calculated by finite difference method.

<sup>b</sup>Using cavity pressure fall time obtained by experiment.

<sup>c</sup>From radiographs of two bars at each injection pressure.

is promising. The factors which cause deviations from the predictions may now be discussed individually.

#### 4.2. Nucleation

It was assumed that when the residual pressure in the liquid fell to zero a void would be produced. In fact the liquid becomes unstable with respect to the vapour when the pressure in the fluid falls below the vapour pressure of the component of the blend with the lowest boiling point. Thus residual adsorbed water, phthalate ester or impurities may be responsible for creating a void. The negative pressure sometimes associated with the nucleation step for bubble formation [17] was considered to be small because of the sites for heterogeneous nucleation provided by ceramic particles, thus, if nucleation of voids occurred in the region  $\pm 0.1$  MPa absolute, the error in taking this threshold pressure as zero by comparison with the injection pressures explored of 10 to 100 MPa is negligible.

#### 4.3. Sprue closure

In each case the calculation underestimates the injection pressure needed to produce moulded bars without voids. One reason for this is to be found in greater comprehension of what is meant by sprue closure. The final stage of mould filling must be seen as a dynamic rather than a static process and the point at which cavity pressure starts to fall is defined by the failure of mass transport by flow along a shrinking cylindrical channel in the sprue to compensate for shrinkage of the molten core. The analysis of final stage filling therefore involves consideration of the dependence of viscosity on temperature and shear rate and is discussed elsewhere [9]. For the suspension used in the present study, the fall in pressure significantly precedes calculated sprue solidification time and this is clearly seen in Fig. 6 on which is marked the calculated sprue solidification time defined by the axis temperature reaching  $T_g$ . For the moulding conditions of series 1, 2 and 3, the times of initial cavity pressure fall, obtained from the cavity pressure traces were 5, 5 and 15 sec, respectively. The increase in mould temperature had very little effect on this time as previously noted [5]. These times are considerably shorter than the time for the axis of the sprue to reach  $T_g$ .

Substituting these experimental values based on cavity pressure drop for sprue closure enabled a new

set of residual pressure against injection pressure curves to be calculated and these are shown in Fig. 7. The calculated threshold injection cavity pressures for the nucleation of voids are given in Table III. For series 1 mouldings with a small sprue and mould temperature of 25 °C, the agreement falls within the bounds defined by the moulding experiment but a significant overestimate is now observed for the series 3 mouldings made at 25 °C with a large sprue. In fact these two estimates of sprue closure time represent upper and lower bounds of a continuous process of final stage mould packing and the corresponding predictions, therefore, tend to under and over estimate the threshold pressure for void formation respectively. A full analysis of the dynamic process of final stage mould packing would have made the computation extremely complex and would demand considerably more material property data.

#### 4.4. Collapse of the walls of the moulding

In the calculations described above, the walls of the moulded bar were assumed to be rigid at the time when sprue closure occurred. The temperature of material at the edge of the bar was calculated as a function of time after injection. The time required for this temperature to reach  $T_g$  was noted for each moulding series and this can be used as an estimate of the minimum time taken for the mould walls to become rigid.

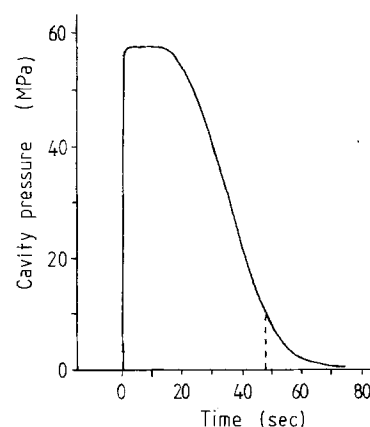


Figure 6 Typical cavity pressure trace for series 3 mouldings showing the predicted sprue solidification time.

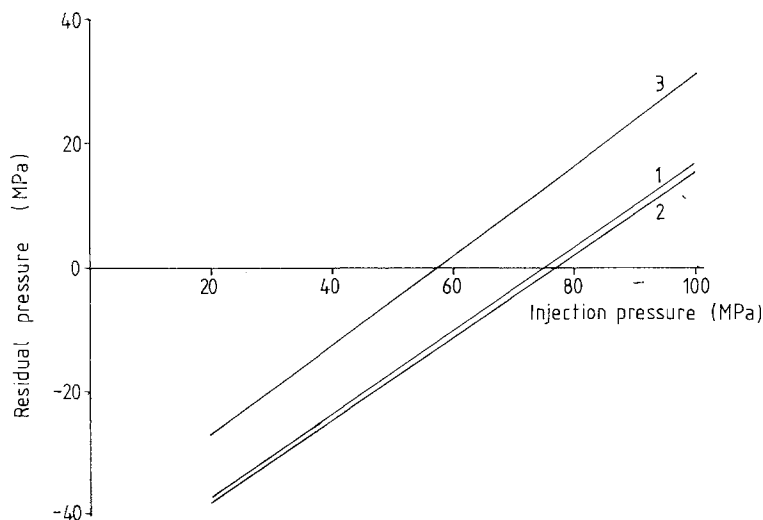


Figure 7 Predicted residual pressure as a function of injection pressure for series 1, 2 and 3 mouldings obtained using measured cavity pressure fall off times.

For a mould temperature of 25 °C the predicted time for the mould walls to solidify was 20 sec. Clearly, this exceeds the time at which cavity pressure starts to fall, namely 5 and 15 sec for the small and large sprue, respectively. For sinking deformation to occur in preference to void formation, however, the time taken for the mould walls to become rigid should be compared with the time taken for residual pressure in the centre of the moulding to fall to zero.

For an injection cavity pressure of 50 MPa the times for the residual pressure to fall below zero were estimated using the procedure in Section 3.1 to be 70 and 116 sec for the small and large sprues, respectively, at a mould temperature of 25 °C. Thus the mould walls are predicted to become rigid well before internal pressure falls to zero and sinking deformation should not occur. Nevertheless some signs of sinking deformation were detected in all the bars moulded with the small sprue. This may have led to the threshold injection pressure being lower experimentally than predicted, this is because the sinking deformation compensates for the shrinkage of the molten core.

There are two possible causes of the sinking deformation observed. It may have been the result of buckling of the skin of the moulded bar under the influence of stresses arising from differential contraction at a stage when the internal pressure was low. It may also indicate that the heat transfer coefficient is not, in reality, high throughout the entire solidification process, or indeed at all points on the surface of the bar. If the bar is able to separate locally from the

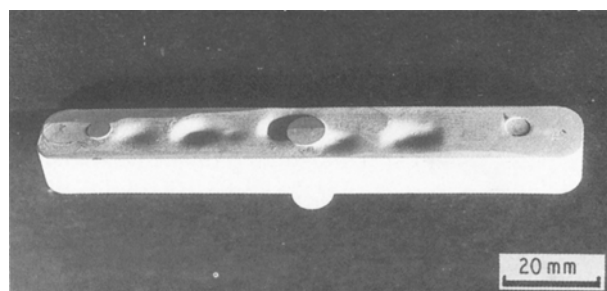


Figure 8 Sink marks in a bar prepared using series 2 moulding conditions.

wall of the mould during shrinkage  $h$  could fall below the value of  $1000 \text{ W m}^{-2} \text{ K}^{-1}$  used in the calculation.

For the series 2 mouldings made at a mould temperature of 46 °C the time taken for an injection pressure of 50 MPa to decay to zero was calculated to be 72 sec and the minimum time taken for the layer next to the wall to solidify was 63 sec. In this case the walls of the moulding were not sufficiently rigid to support the formation of voids as zero pressure was reached and so large sink marks were created and are clearly visible in Fig. 8. Voids could also be created at a later stage when the solid wall thickened.

#### 4.5. The effect of shear heating and cooling during mould filling.

The present study has been concerned only with solidification and has not considered the filling stage of injection moulding. During the mould filling stage, heat may be generated by viscous flow and heat may also be lost to the mould. No attempt has been made here to quantify these processes, however, their effect on the predictions can be judged by calculating the residual pressure as a function injection temperature.

For example, Fig. 9 shows the predicted variation of residual pressure with injection temperature for material moulded with a mould temperature of 25 °C, an injection pressure of 50 MPa and a constant sprue cut off time of 5 sec. The shear heating and cooling would also affect the sprue cut off time but for the purpose of this calculation this value was kept constant. From this curve it can be seen that the effect of cooling is to reduce the likelihood of voiding and that the effect of shear heating caused by the rapid injection of high viscosity material is to increase the likelihood of voiding. A variation of residual pressure of 3 MPa for a 10 °C variation in injection temperature is significant though not large.

#### 4.6. Effect of pressure on $T_g$

The principal effect of pressure on material properties in the present study is the increase in  $T_g$  with pressure for polymers. The effect of varying  $T_g$  while keeping all other parameters constant is shown in Fig. 10 for

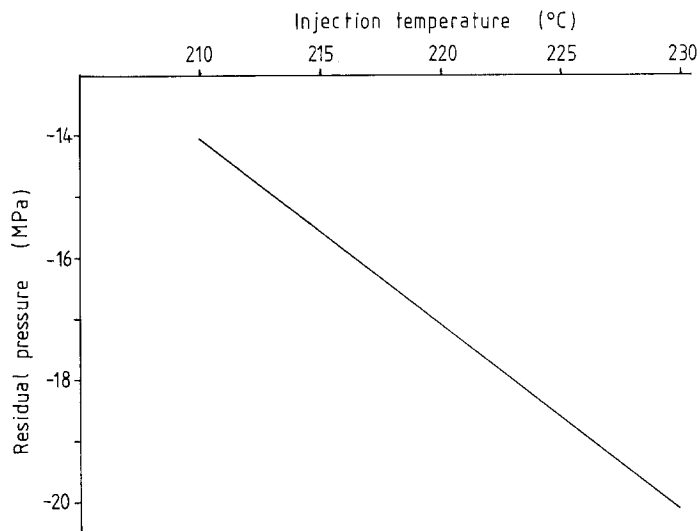


Figure 9 Predicted residual pressure plotted against injection temperature for the polystyrene-zirconia suspension moulded at 50 MPa pressure with mould temperature of 25 °C and sprue cut off time 5 sec.

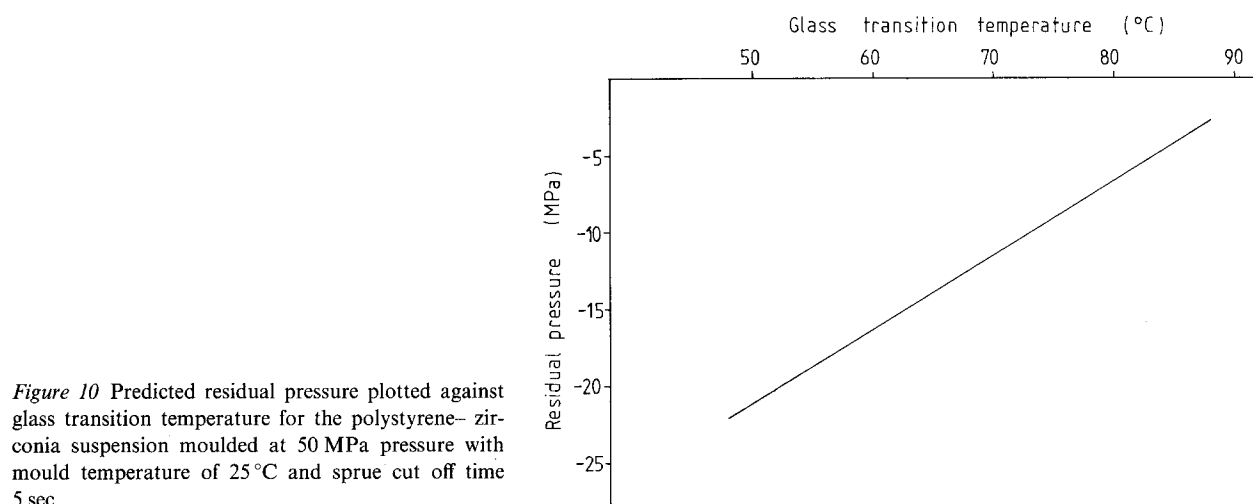


Figure 10 Predicted residual pressure plotted against glass transition temperature for the polystyrene-zirconia suspension moulded at 50 MPa pressure with mould temperature of 25 °C and sprue cut off time 5 sec.

material moulded at 50 MPa with injection temperature 220 °C, mould temperature 25 °C and sprue cut off time 5 sec. For unplasticized polystyrene at 50 MPa  $T_g$  may increase by 16 °C [18]. An increase in  $T_g$  of 16 °C in the composite under consideration increases the predicted residual pressure by 7.6 MPa, however, this is a considerable oversimplification in the calculation, for in reality,  $T_g$  should change with each time step as pressure changes. The effect of the pressure dependence of  $T_g$  is not, therefore, expected to be as large as this.

#### 4.7. The effect of heat transfer coefficient

Assigning a single value for the surface heat transfer coefficient between material and mould is obviously a simplification. The heat transfer coefficient is dependent upon the contact at the wall, the location of cooling channels in the mould and the mould material and surface finish.

The effect that the uncertainty in the value of heat transfer coefficient  $h$  has on the results may be judged by predicting the residual pressure for material moulded at 50 MPa with a mould temperature 25 °C, injection temperature 220 °C and constant sprue cut off time of 5 sec for a wide range of values of heat

transfer coefficient. For  $h = 100 \text{ W m}^{-2} \text{ K}^{-1}$  the residual pressure was  $-23.6 \text{ MPa}$ , for  $h = 1000 \text{ W m}^{-2} \text{ K}^{-1}$  the residual pressure was  $-17.1 \text{ MPa}$  and for  $h = 2000 \text{ W m}^{-2} \text{ K}^{-1}$  the residual pressure was  $-14.4 \text{ MPa}$ . The effect that  $h$  may have on the sprue cut off time was not considered since unlike the moulding the sprue tends to be held against the mould wall by pressure on material.

The results indicate that while  $h$  may affect the solidification time for the moulding, the effect of very wide variations in  $h$  on the incidence of voids is small.

#### 4.8. Errors introduced in the calculation of residual pressure.

The residual pressure was calculated by taking the average specific volume in the core region when the sprue solidified and setting the temperature equal to  $T_g$ . A more rigorous approach would be to calculate the pressure and specific volume in each volume element at times  $t + \Delta t$  after the sprue has solidified from the pressure and specific volumes in the same volume elements at times  $t$ .

Mass transport occurs between one volume element and another as the solidifying front approaches the centre of the bar, therefore, at any time after the sprue

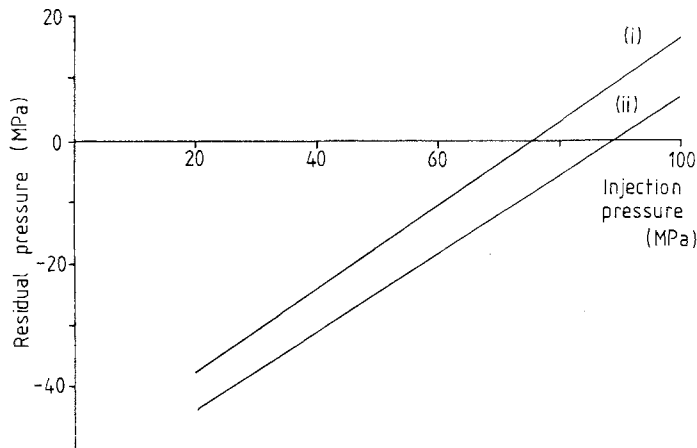


Figure 11 Predicted residual pressure as a function of injection pressure for material moulded with mould temperature 25 °C and sprue cut off time 5 sec considering (i) the average specific volume and (ii) the specific volume of the central region when calculating the residual pressure.

has solidified, both the pressure and specific volume in each volume element are unknown, i.e.  $N$  specific volumes and the pressure are unknown.  $N$  equations can be written balancing the equation of state in each element at times  $t + \Delta t$  with those at times  $t$ . A further equation is required and may be obtained from the assumption that the volume occupied by the core region when the sprue solidifies is invariant. The shrinkage of the solidified layers could also be included in this equation.

These equations would need to be solved after each time step until the complete bar was solid or until zero pressure was reached. This is obviously a very complex procedure and would require a considerable amount of computing time. The loss of accuracy incurred by the less rigorous procedure must be set against the simplification to a computer model intended for the predictive exploration of ceramic injection moulding parameters and is discussed below.

The error is introduced by using the average specific volume of the molten core when the sprue solidifies to calculate the residual pressure. In order to assess this error the specific volume of a small central region, calculated at the sprue solidification time, was used instead. The voids observed are approximately 2 mm across so a central area of 4 or 1 mm<sup>2</sup> in the quarter bar was considered appropriate. Fig. 11 shows residual pressure against injection pressure curves for material moulded with mould temperature 25 °C and sprue cut off time 5 sec using (i) the average specific volume and (ii) the specific volume of this central area. The critical injection pressure for a zero residual pressure is 14 MPa higher in case (ii). This is a significant difference but results from the extreme case of assuming no mass transport within the core during solidification. The real error caused by taking the average specific volume will be smaller than this.

## 5. Conclusions

A finite difference two-dimensional unsteady state heat transfer numerical method has been applied to the problem of solidification of a simple injection moulded ceramic body. The equation of state for the suspension was known and hence it was possible to calculate the residual pressure just prior to solidi-

fication of the final pool of liquid, as a function of hold pressure applied by the injection moulding machine. Thus voids were predicted to occur at the centre of mouldings where the residual pressure fell to zero. The success of this prediction depended critically on two other factors: the value taken for sprue closure time and the value of wall temperature for the moulding at the point when the pressure in the core of the moulding fell below zero. For the former, upper and lower limits are given by the time for the sprue axis temperature to reach  $T_g$  which may be obtained by calculation and the time for initial cavity pressure drop obtained experimentally. These values offer lower and upper bounds of the threshold pressure, respectively. If the wall temperature is significantly above the softening point of the material at the time when pressure falls to zero then collapse of the wall of the moulding may take preference over the evolution of voids. The errors in the procedure have been assessed and set against the simplifications in computing that result. The procedure allows a predictive analysis of the affect of a wide range of material and machine parameters on the integrity of mouldings.

## Acknowledgements

The authors are grateful to SERC for supporting the ceramic fabrication programme and to T & N Technology for supplying the zirconia powder.

## References

1. M. J. EDIRISINGHE and J. R. G. EVANS, *Int. J. High. Tech. Ceram.* **2** (1986) 1.
2. *Idem. ibid.* **2** (1986) 249.
3. J. G. ZHANG, M. J. EDIRISINGHE and J. R. G. EVANS, *Ind. Ceram.* **9** (1989) 72.
4. M. J. EDIRISINGHE and J. R. G. EVANS, *J. Mater. Sci.* **22** (1987) 2267.
5. J. G. ZHANG, M. J. EDIRISINGHE and J. R. G. EVANS, *ibid.* **24** (1989) 840.
6. M. S. THOMAS and J. R. G. EVANS, *Brit. Ceram. Trans. J.* **87** (1988) 22.
7. K. N. HUNT, J. R. G. EVANS, J. WOODTHORPE, *J. Mater. Sci.* in press.
8. *Idem., ibid.* in press.
9. *Idem., ibid.* in press.
10. F. KREITH and M. S. BOHN, "Principles of Heat Transfer", 4th edn (Harper and Row, New York, 1986) pp 158–167.



11. B. CARNAHAN, H. A. LUTHER, and J. O. WILKES, "Applied Numerical Methods" (Wiley, New York, 1969), pp. 452-461.
12. N. J. MILLS, *J. Mater. Sci.* **17** (1982) 558.
13. M. J. EDIRISINGHE, *J. Mater. Sci. Lett.* **7** (1988) 509.
14. N. J. MILLS, Private Communication.
15. M. R. KAMAL and S. KENIG, *Soc. Plast. Eng. J.* **26** (1970) 50.
16. M. RIGDAHL, *Int. J. Polym. Mater.* **5** (1976) 43.
17. H. N. V. TEMPERLEY, "Properties of Matter", Third Edn (University Tutorial Press, London) pp 231-237.
18. M. C. SHEN and A. EISENBERG, "Progress in Solid State Chemistry", Vol. 3, edited by H. Reiss (Pergamon, Oxford, 1966), p. 456.

*Received 18 September 1989  
and accepted 19 February 1990*